HUMAN VACCINES & IMMUNOTHERAPEUTICS
2017, VOL. 13, NO. 7, 1586–1597
https://doi.org/10.1080/21645515.2017.1295190

Taylor & Francis
Taylor & Francis Group

RESEARCH PAPER

Novel recombinant DNA vaccine candidates for human respiratory syncytial virus: Preclinical evaluation of immunogenicity and protection efficiency

Mohamed A. Farrag[a], Haitham M. Amer[a,b], Peter Öhlschläger[c], Maaweya E. Hamad[a], and Fahad N. Almajhdi[a]

[a]Department of Botany and Microbiology, College of Science, King Saud University, Riyadh, Saudi Arabia; [b]Department of Virology, Faculty of Veterinary Medicine, Cairo University, Giza, Egypt; [c]Institute of Nano- and Biotechnology, Department of Chemistry and Biotechnology, Aachen University of Applied Sciences, Juelich, Germany

ABSTRACT

The development of safe and potent vaccines for human respiratory syncytial virus (HRSV) is still a challenge for researchers worldwide. DNA-based immunization is currently a promising approach that has been used to generate human vaccines for different age groups. In this study, novel HRSV DNA vaccine candidates were generated and preclinically tested in BALB/c mice. Three different versions of the codon-optimized HRSV fusion (F) gene were individually cloned into the pPOE vector. The new recombinant vectors either express full-length (pPOE-F), secretory (pPOE-TF), or $M2_{82-90}$ linked (pPOE-FM2) forms of the F protein. Distinctive expression of the F protein was identified in HEp-2 cells transfected with the different recombinant vectors using ELISA and immunofluorescence. Mice immunization verified the potential for recombinant vectors to elicit significant levels of neutralizing antibodies and $CD8^+$ T-cell lymphocytes. pPOE-TF showed higher levels of gene expression in cell culture and better induction of the humoral and cellular immune responses. Following virus challenge, mice that had been immunized with the recombinant vectors were able to control virus replication and displayed lower inflammation compared with mice immunized with empty pPOE vector or formalin-inactivated HRSV vaccine. Moreover, pulmonary cytokine profiles of mice immunized with the 3 recombinant vectors were similar to those of the mock infected group. In conclusion, recombinant pPOE vectors are promising HRSV vaccine candidates in terms of their safety, immunogenicity and protective efficiency. These data encourage further evaluation in phase I clinical trials.

ARTICLE HISTORY
Received 28 November 2016
Revised 2 February 2017
Accepted 9 February 2017

KEYWORDS
DNA vaccine; disease enhancement; fusion protein; human respiratory syncytial virus; pPOE vector; truncated form

Introduction

Human respiratory syncytial virus (HRSV) is associated with severe lower respiratory tract disease in infants, young children and the elderly.[1,2] Disease progression and complications are more severe in children with underlying cardiopulmonary disease and immuno-compromised adults. Recurrent infections are common due to the inability of natural infection to establish long lasting immunity.[3,4] A substantial disease impact was recorded in both developed and developing countries. Worldwide estimations have indicated that HRSV infects more than 33 million children each year, 3.4 million of whom have been hospitalized and 200,000 have died.[1] The annual burden of HRSV infections in the USA only was estimated at 2.8 billion US $ for children[5] and 1 billion US $ for the elderly.[6] Despite its significance, no licensed vaccines are available to control HRSV outbreaks.[7] The failure to validate an HRSV vaccine to date is attributed to the incomplete immunity of vaccine candidates, the lack of neutralizing antibodies, and the limited $CD8^+$ T cell response.[8]

HRSV is a primary member of the genus *Orthopneumovirus* and the family *Pneumoviridae*.[9] The viral genome comprises a single molecule of negative RNA that encodes 11 structural and non-structural proteins.[10] Two surface glycoproteins, attachment (G) and fusion (F), were described as principal targets for host immunity.[11] The F protein was highly recommended for use in the development of vaccine candidates due to its conserved nature and ability to induce neutralizing antibodies and cytotoxic T lymphocytes.[12,13] A number of HRSV vaccine candidates were generated and tested in preclinical and/or clinical trials including FI-RSV,[14] live-attenuated,[15] subunit[16] and viral vector-based[17] vaccines. FI-RSV was prohibited due to its hazardous effect, which resulted in disease enhancement and the death of 2 vaccine recipients.[14] Such effects were attributed to the Th-2-biased immune response and pulmonary eosinophilia.[18] Other vaccine preparations had important limitations, which lessened their significance. These limitations included instability, the inefficient replication and risk of reversion of live-attenuated virus vaccines.[7,15] and denaturation associated with the purification of subunit vaccines.[19]

Naked DNA immunization is considered a promising approach for the generation of safe and potent vaccine candidates owing to its superior attributes. These include the ease of construction, high-insertion capacity, non-immunogenic nature of the vector, proper post-translational modifications, and induction of both humoral

CONTACT Fahad N. Almajhdi majhdi@ksu.edu.sa Department of Botany and Microbiology, College of Science, King Saud University, Riyadh 11451, Saudi Arabia, P.O. Box 2455.

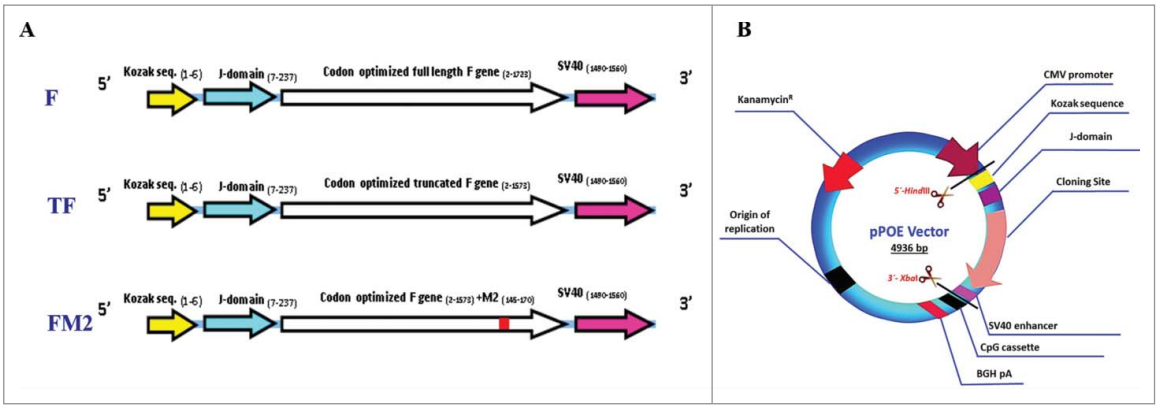

Figure 1. (A) Schematic representation of the different HRSV F gene cassettes. Three versions of the F gene were codon optimized to the human system. The Kozak sequence and J-domain were linked to the 5′-end and the SV40 enhancer sequence was added to the 3′-end. (B) Recombinant pPOE immunization vector. The diagram shows the structural components of the vector and their relative positions including the origin of replication (ori), kanamycin resistant gene (kan) for selection of recombinant clones, CMV promoter for mammalian gene expression, and CpG cassette for activation of the Toll-like receptor-9 signaling cascade. The cloning site of F gene cassette is indicated.

and cellular immune responses. Moreover, the production costs are relatively low, and the DNA is stable and does not require refrigeration for storage.[20,21] Several DNA vaccine formulations containing the F, G and matrix protein (M2) either alone or in combination were tested in animal models.[220-26] these formulations were capable of stimulating the production of neutralizing antibodies, cytotoxic T lymphocytes and IFN-γ and conferring protection upon viral challenge. However, the lower level of transgene expression and the need for large doses to evoke robust immune response require further improvements in the design of vaccine candidates.[27] Several investigators showed that the immunogenicity of DNA vaccines was significantly enhanced by the incorporation of CpG motifs[28] and/or cytokine genes[29] in the vector backbone.

In the current study, 3 different versions of the codon optimized HRSV F gene were individually cloned into the novel expression vector pPOE, which contains enhancer sequences such as a CpG motif, J-domain and SV40 enhancer for powerful gene expression and immune response (Fig. 1).[30] The expression potential of recombinant pPOE vectors was evaluated via the transfection of HEp-2 cells, whereas the immunogenicity was studied in BALB/c mice. Virus challenge of immunized mice was undertaken to ensure safety and protective efficiency of the recombinant vectors.

Results

Recombinant pPOE vectors induced robust in vitro *expression of F protein*

The ability of recombinant pPOE vectors to express F protein; derived from the wild-type virus (Riyadh 91/2009), in HEp-2 cells was verified using quantitative ELISA and direct immunofluorescence. Significant concentrations of the F protein were identified in the wells transfected with the recombinant pPOE vectors compared with the negative control wells by ELISA (1.435 $\pm$ 0.12 μg/ml; $P = 0.002$ for pPOE-F, 3.478 $\pm$ 0.08 μg/ml; $P = 0.0002$ for pPOE-TF and 2.747 $\pm$ 0.14 μg/ml; $P = 0.001$ for pPOE-FM2). In contrast, cells transfected with the recombinant pPOE vectors showed diffuse intracytoplasmic fluorescence staining using HRSV-specific FITC conjugated antibodies. Negative control wells showed no specific fluorescence signals. Cells transfected with pPOE-TF vector displayed the highest fluorescence reactivity in terms of intensity and spread.

Recombinant pPOE vectors provoked significant antibody response in mice

The immunogenicity of recombinant pPOE vectors in mice was evaluated by determining the rise in serum levels of HRSV F-specific antibodies (IgG and IgA) before and after immunization. Two sera samples were collected from the groups of mice at days 0 and 20 (i.e., before immunization and 10 d after the 2nd immunization). Antibody detection ELISA has revealed that there were no F-specific antibodies in the mice sera of any group at day 0. Similarly, no antibodies were detected at day 20 in the mice immunized with pPOE and in the mock-immunized group. The mice immunized with pPOE-TF showed an induction of high levels of IgG and IgA at day 20, with mean OD values of 0.583 $\pm$ 0.039, $P < 0.0001$, and 0.256 $\pm$ 0.03, $P < 0.001$, respectively. Both pPOE-F and pPOE-FM2 elicited reasonable antibody levels with mean OD values of 0.310 $\pm$ 0.018 with $P < 0.0001$ (IgG) and 0.169 $\pm$ 0.025 with $P = 0.001$ (IgA) for pPOE-F, and 0.322 $\pm$ 0.018 with $P < 0.0001$ (IgG) and 0.159 $\pm$ 0.01 with $P < 0.0001$ (IgA) for pPOE-FM2 (Fig. 2A). The neutralizing activity of the raised antibodies was evaluated by a micro-neutralization assay. Mice immunized with pPOE-TF developed the highest level of neutralizing antibody titer (5.5 $\pm$ 0.58 log 2) compared with pPOE-F and pPOE-FM2 immunized mice (4.5 $\pm$ 0.58 log2 and 4.75 $\pm$ 0.5 log2, respectively).

Immunization with recombinant pPOE vectors elicited potent CTL activities

Cellular immunity was additionally monitored 10 d after the 2nd immunization by measuring IFN-γ and granzyme B secretion of stimulated splenocytes *ex vivo*. All recombinant pPOE vectors induced robust IFN-γ and granzyme B responses compared with the empty pPOE vector (IFN-γ: 2.95 $\pm$ 1.24 spots/

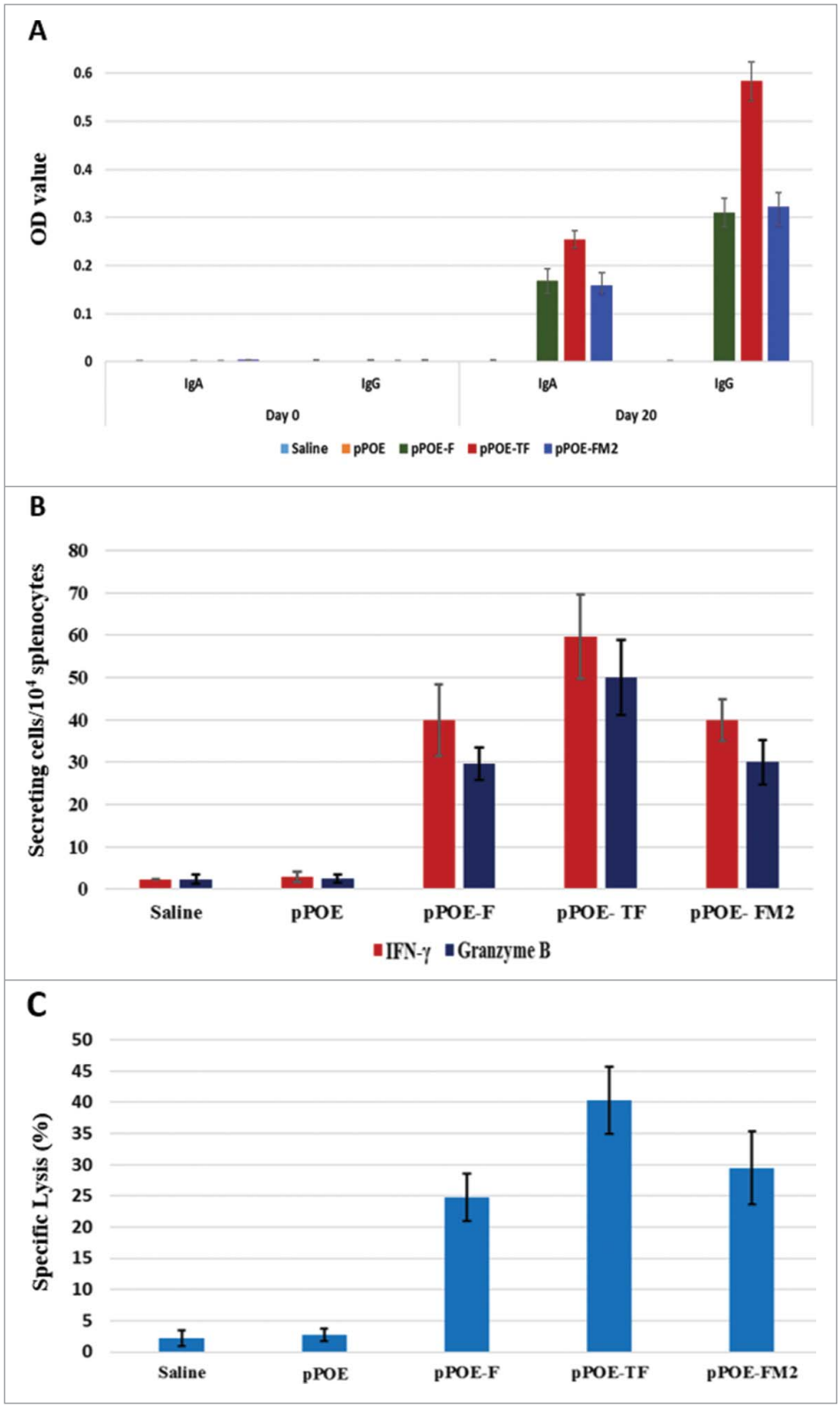

Figure 2. A) HRSV F-specific IgA and IgG levels in sera of the immunized groups of mice at days 0 and 20. The bars show the mean optical densities (OD) ± standard deviation (SD). B) The *ex vivo* IFN-γ and granzyme B secretion of stimulated splenocytes as measured by Elispot assays. The bars show the mean spot number per 1×10^4 splenocytes ± SD. C) The *ex vivo* ^{51}Cr release assay for lysis of peptide loaded target cells. The bars show the mean percentages of specific lysis ± SD. The collective data of 2 independent experiments are shown.

10^4 splenocytes, granzyme B: 3.25 ± 1.03 spots/10^4 splenocytes). The number of spots induced by the pPOE-F and pPOE-FM2 vectors was similar (IFN-γ: 40 ± 8.4; $P < 0.01$ and 40 ± 4.95; $P < 0.001$, respectively and Granzyme B: 29.6 ± 3.9; $P < 0.0001$ and 30 ± 5.3; $P < 0.001$, respectively). However, splenocytes of pPOE-TF immunized mice revealed the highest responses to IFN-γ (59.6 ± 10 $P < 0.01$) and granzyme B (50 ± 8.9; $P < 0.001$) (Fig. 2B). P values were calculated

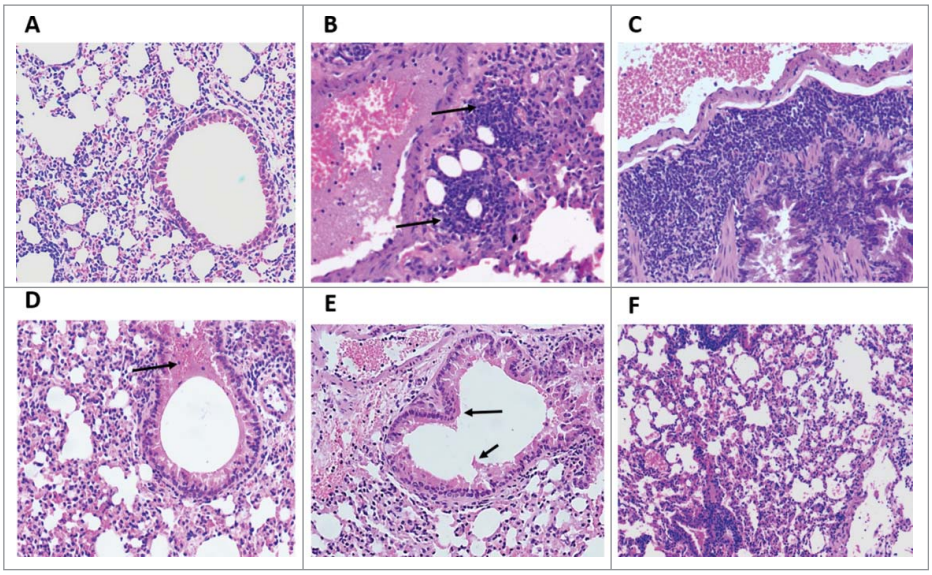

Figure 3. Histopathological findings in the lungs of immunized mice at 8 d post-challenge. Lung sections were stained with haematoxylin and Eosin and were examined using an Eclipse E-800 microscope (Nikon). Images were captured with a DXM1200C digital camera at a magnification power of 200X. Lung sections of mock-infected mice showed no infiltration of inflammatory cells – Score 0 (A). Lung sections of mice immunized with empty pPOE vector showed focal peribronchial leukocytic aggregations (arrows) – Score 2 (B), and those of FI-RSV immunized mice displayed massive infiltration of leukocytes with several layers of infiltrating cells and airway restriction – Score 3 (C). The lung sections of mice immunized with pPOE-F (D), pPOE-TF (E), and pPOE-FM2 (F) showed few leukocytes infiltrating in the peribronchiolar space and polypoids of the epithelial lining (arrows) – Score 1.

compared with the spots developed by the mock-immunized group of mice.

Further analysis of the cellular immune response by a ^{51}Cr release assay was conducted to determine the cytolytic activity of F-specific CTLs. In agreement with the results of the Elispot assays, splenocytes of the mice immunized with the recombinant pPOE vectors showed strong lysis of RMA-S cells loaded with the $F_{85–93}$ peptide. pPOE-TF vector mediated the highest cytolytic activity (40.37% ± 5.37 $P < 0.001$) compared with pPOE-F and pPOE-FM2 (24.75 ± 3.77; $P < 0.001$ and 29.5 ± 5.87; $P < 0.001$, respectively). Poor lysis activity was described in mice immunized with the empty pPOE vector (2.75 ± 1.03) and in the mock-immunized group (2.25 ± 1.28) (Fig. 2C).

Mice immunization with recombinant pPOE vectors controlled virus replication in lungs and reduced airway inflammation post-challenge

Evaluating the competence of recombinant pPOE vectors in protecting immunized mice from challenge with wild-type virus (Riyadh 91/2009) was clinically indistinctive. All tested groups of mice did not develop apparent clinical signs, and no mortalities were recorded. At the 8th day post-challenge, lungs were extirpated from the immunized mice to measure the viral load and evaluate the extent of inflammatory response in the lung tissue. End-point titration indicated that the virus titer in groups of mice immunized with the recombinant pPOE vectors was $10^{3.5}$, $10^{2.8}$ and $10^{3.0}$ $TCID_{50}$/gram of lung tissue for pPOE-F, pPOE-TF and pPOE-FM2, respectively. More relevant viral loads were identified in the lungs of FI-RSV immunized mice ($10^{3.7}$ $TCID_{50}$/gram lung tissues). Mice immunized with empty pPOE vector displayed a titer of $10^{5.6}$ $TCID_{50}$/gram of lung tissues, whereas the mock-infected group did not show any signs of virus replication. Histological examination of stained lung sections has revealed extensive pathologic abnormalities in the lungs of FI-RSV immunized mice (Score 3). These abnormalities included focal alveolar collapse with excessive peribronchial and perivascular leukocytic infiltration (mainly lymphocyte and plasma cells), and obstruction of the bronchiolar lumen with a mixture of inflammatory and necrotic cells. Mice that had been immunized with pPOE vector showed moderate airway inflammation with focal peribronchial aggregation of the infiltrating leukocytes (Score 2). Less severe inflammation was observed in the lungs of mice immunized with recombinant pPOE vectors. Few leukocytes were found around the bronchioles and the blood vessels with polypoids in the bronchial epithelial lining (Score 1). No signs of inflammation were observed in the mock-infected group (Score 0) (Fig. 3).

Mice immunized with recombinant pPOE vectors displayed lung cytokine profiles comparable to mock-infected group

The lung cytokine profile of immunized mice was measured 8 d post-challenge to evaluate the capacity of recombinant pPOE vectors in stimulating a safe immune response. RNA was extracted and cDNA was synthesized for use as a template to generate Th1/Th2 gene expression profiles for each group of mice by using RT^2-PCR Profiler arrays. The Ct values were normalized against the HKGs provided by the array, and the mock-infected group was set as a control for data analysis. Samples that exceeded a 2-fold change in gene expression were considered for further evaluation.

The cytokine profiles of the mice immunized with FI-RSV and empty pPOE vector consisted of a mixture of Th1 and Th2 responses. The FI-RSV group showed a marked increase in Th2 response with substantial upregulation of 16 of the 18 Th2-associated genes (fold change values ranged from 10.27

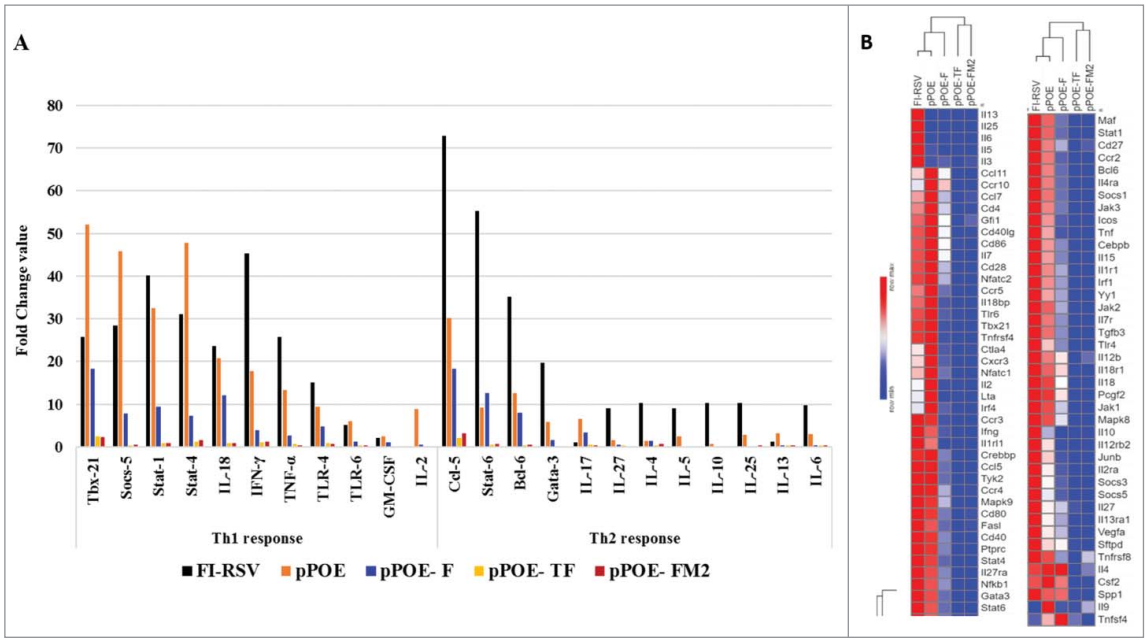

Figure 4. A) Gene expression of key cytokines involved in Th1 and Th2 responses. The lungs of the different groups of mice were harvested 8 days' post-challenge and the RNA extracts were tested by a RT^2-PCR Profiler Array (Qiagen). The columns show fold change values of each cytokine. B) Lung cytokine profile heatmap of immunized groups of mice. The heatmaps were generated using the MORPHEUS software tool. The rows were sorted in ascending gene expression order and were processed for hierarchical clustering using one minus Pearson's correlation. The gradient from blue to red indicates minimum to maximum expression of the indicated genes. The clustering of the groups of mice is shown above the columns.

for IL-4 to 72.84 for Ccl$^-$5). The majority of the Th-1 associated genes (17 of 19) were upregulated to a lesser extent (fold change values ranged from 2.10 for GM-CSF to 47.33 for Socs-5). Alternatively, the group of mice immunized with empty pPOE vector showed a Th1-biased response with a distinctive upregulation of 18 Th1-associated genes (fold change values ranged from 8.9 for IL-2 to 51.99 for Tbx-21). Only 9 Th2-associated genes were upregulated in the pPOE group (fold change values ranged from 2.86 for Ccr-4 to 30.28 for Ccl$^-$5) (Fig. 4).

In contrast, mice immunized with the pPOE-TF or pPOE-FM2 vectors have cytokine expression profiles very close to that displayed by the mock-infected group. Only 2 genes were upregulated in both groups; Ccl$^-$5 (fold changes: 2.07 and 3.21, respectively) and Tbx-21 (fold changes: 2.44 and 2.26, respectively). For the pPOE-F group, 71 of the 84 genes were upregulated (23 genes $\geq$ 5-folds and 36 genes $\geq$ 2-folds). The fold increase in the Th1-associated genes (Tbx-21:18.38, Stat-4:7.2, Ccr-5:3.64, IFN-γ:3.9, Cxcr-3:6.2, Stat-1:9.4, IL-18:12.14) was much higher than that in Th2-associated genes (Gata3:1.6, Ccr-4:1.3, IL-6:0.27, IL13:0.38, IL-25:0.23, IL-10:0.03, IL-27:0.46, IL-5:0.04, IL-4:1.39) (Fig. 4).

The effect of mice immunization on disease progression post-challenge was further analyzed by monitoring the expression level of genes involved in the TLR signaling pathway, eosinophil migration, acute inflammatory response and cellular immunity. FI-RSV and pPOE immunized mice exhibited upregulation of all genes contributing to disease enhancement, with higher fold change values for the former. However, these genes were marginally upregulated, downregulated or remained unchanged in mice immunized with pPOE-TF and pPOE-FM2 vectors. In pPOE-F immunized mice, 20 of the 25 genes involved in the aforementioned pathways were upregulated, with fold changes distinctly lower than those of the FI-RSV and pPOE groups (Table 1).

Discussion

Lower respiratory tract infections caused by HRSV are still a major public health problem that requires seeking safe and effective vaccines. DNA vaccines are immunogenic and effective in protection against several viral infections, including HRSV.[21,25,26,31] HRSV DNA vaccine candidates that used commercially available plasmid vectors such as pcDNA3.1,[23,32] pET-32,[33] and pVCL1012[34] have variable immunogenicity and the ability to confront virus challenge. A novel immunization vector, which is currently unavailable in the market, was constructed to induce a potent CTL response and tumor regression in mice with cervical cancer[35] or prostate carcinoma.[36] The pPOE vector was designed to permit the introduction of several built-in enhancer sequences that allow better transgene expression and powerful induction of the immune response, including the J-domain, CpG motif and SV40 enhancer. The J-domain is known to mediate the MHC-I cross-presentation and priming of CD8$^+$ T cells, which are crucial for HRSV clearance.[37] CpG activates the TLR-9 cascade and mediates interferon production via a MyD88-dependent pathway.[38] The SV40 enhancer increases nuclear uptake, particularly in non-dividing cells,[39] increases transgene expression[40] and potentiates the antibody response.[41]

The F protein, a type 1 viral protein, has long been considered the most promising target for developing DNA vaccine candidates against HRSV due to its conserved nature and its ability to activate both the humoral and cellular immune responses.[42] However, the use of the non-optimized F gene in DNA vaccination has provided unsatisfactory protection in

Table 1. Fold-change expression of the genes associated with the immunologic pathways of disease progression in the lungs of immunized mice compared with the mock infected group.

		Fold change values				
	Gene name	FI-RSV	pPOE	pPOE- F	pPOE- TF	pPOE- FM2
TLR signaling pathway						
IRF-1	Interferon regulatory factor 1	20.54	15.04	7.15	1.11	1.09
IRF-4	Interferon regulatory factor 4	6.65	14.55	2.83	0.45	0.24
TLR-4	Toll-like receptor 4	15.00	9.47	4.72	0.77	0.73
TLR-6	Toll-like receptor 6	5.21	6.02	1.19	0.41	0.25
GFI-1	Growth factor independent 1	3.02	3.65	1.96	0.26	0.94
Eosinophils migration						
Ccl¯5	Chemokine (C-C motif) ligand 5	72.84	30.28	18.22	2.07	3.21
Ccr-2	Chemokine (C-C motif) receptor 2	28.07	21.33	5.24	0.29	0.20
Ccl¯7	Chemokine (C-C motif) ligand 7	3.65	4.98	2.28	0.70	1.03
Ccr-3	Chemokine (C-C motif) receptor 3	21.87	20.34	2.46	0.49	0.61
Ccl¯11	Chemokine (C-C motif) ligand 11	8.94	3.24	3.32	0.61	0.61
Acute inflammatory response						
TNF-α	Tumor necrosis factor- α	25.67	13.28	2.64	0.62	0.39
IL-6	Interleukin 6	9.66	2.98	0.27	0.41	0.28
GM-CSF	Colony stimulating factor 2 (granulocyte-macrophage)	2.10	2.45	0.98	0.12	0.20
Ccr-5	Chemokine (C-C motif) receptor 5	11.61	15.25	3.63	0.39	0.22
Spp-1	Secreted phosphoprotein 1	7.90	6.61	6.34	0.79	0.43
TNF-β	Tumor necrosis factor-β	3.74	7.65	0.50	0.48	0.36
Cellular mediated Immunity						
CD4	CD4 Antigen	24.41	32.74	13.81	0.67	1.81
CD45	CD45 Antigen	19.30	17.78	6.08	1.34	1.64
Tyk2	Tyrosine Kinase 2	16.00	16.07	3.97	0.62	0.51
Fasl	Fas 1 ligand	15.91	13.36	3.74	0.38	1.45
Cd86	CD86 Antigen	10.58	12.35	6.75	1.53	1.00
Cd80	CD80 Antigen	9.26	8.36	2.39	0.12	0.88
Cd28	CD28 Antigen	7.97	9.22	3.57	0.24	0.49
Cd40	CD40 Antigen	12.76	11.69	3.97	0.59	0.90
Cd40lg	CD40 Ligand	5.89	6.91	3.49	0.32	0.63

mice.[27] The reason for this incompetence is the presence of premature polyadenylation signals that hinder F protein expression. Codon optimization was recommended to remove such signals and enhance codon usage.[22] Removal of the transmembrane domain also provided superior immunogenicity *in vivo* compared with the full-length F gene.[43,44] Expression of the immuno-dominant epitope of the HRSV M2 protein (residues 82–90) in conjunction with the F or G proteins induced a potent CTL response and a balanced Th1/Th2 response in mice.[37,45] Therefore, we chose 3 different versions of the codon optimized HRSV F protein gene to be evaluated in mice after cloning into the pPOE vector. These recombinant vectors express full (pPOE-F), secretory (pPOE-TF) or $M2_{82-90}$ linked (pPOE-FM2) forms of the F gene (Fig. 1).

The expression potential of the 3 recombinant vectors was first analyzed in cell culture before proceeding to *in vivo* studies. Significant levels of F protein were identified in HEp-2 cells using ELISA and immunofluorescence with a higher abundance of the secretory form. The proper expression of these constructs is consistent with the previous trials of DNA immunization using codon optimized and truncated F protein forms[17,23,26,37] It was expected that the secretory form should have the lowest intracellular concentration due to its rapid secretion in the cell supernatant. Harvesting the expressed proteins 48 hr post-transfection, which may be insufficient for protein secretion, can justify this unexpected finding. The F protein is primarily expressed in a pre-fusion form, which is metastable and readily cleaved to the post-fusion form.[46] Both of the F protein forms, particularly the pre-fusion form, induce potent neutralizing antibodies.[47-49] The identification and quantitative measurement of both the F protein forms were not investigated in this study because both forms induce powerful immune responses. However, we expect that a mixture of pre- and post-fusion forms exist in the transfected cells, with the post-fusion form dominating due to its higher stability.

The 2 arms of immunity were analyzed in response to immunization with the 3 recombinant vectors in BALB/c mice. All vectors, particularly pPOE-TF, induced significant levels of neutralizing antibodies and potent $CD8^+$ T cell response (Fig. 2) because of the codon optimization and incorporation of the enhancer sequences in the vector backbone. Previous studies generated similar results in an IFN-γ ELISPOT assay[23,24,50]; however, we also performed granzyme B ELISPOT and ^{51}Cr-release assays to selectively recognize the cytolytic activity of HRSV-specific $CD8^+$ T cells. Although including the $M2_{82-90}$ epitope in immunization against HRSV induced robust $CD8^+$ T cell responses in many studies,[37,45] we did not find significant differences between mice immunized with pPOE-F and pPOE-FM2 (Fig. 2B and C). This may confirm that the enhanced $CD8^+$ T cell activity is principally attributed to sub-dominant epitopes in the F protein.[51]

The vaccination failure against HRSV is attributed to the lower protective efficiency of the vaccine candidate and/or disease enhancement post-challenge due to the Th2-biased immune response.[52] Three parameters were considered for the evaluation of protection and enhanced disease in the current

study, including viral load, histopathological alterations and cytokine profile in the lungs of immunized mice 8 d post-challenge. Although day 8 is a good time-point for assessing enhanced disease, the peak of viral replication is most commonly attained at days 4–6 after infection. Nevertheless, the altered pathogenicity of the virus strain used in the challenge experiments (Riyadh 91/2008) that peaks at days 7–8, as indicated by virus titration, immunofluorescence and real-time RT-PCR (unpublished data) justifies day 8 as a suitable time-point for testing protection and enhanced disease simultaneously. As well, at earlier time-points post-challenge, pulmonary viral loads and cytokine profiles will be very similar among all challenged groups[53] which restrict the possibilities to compare the current data with those reported in published studies. Therefore, late time-point of necropsy can give the immune system more time to control the virus replication and variation between immunized groups will be visible. Pulmonary cytokine profiling did not receive much attention in the literature, although it provides an accurate picture of the immunological response against virus challenge. Few cytokines have been considered for this analysis (mostly IL4 and IFN-γ).[23,31,50] In the current study, we expanded the array to involve 84 genes associated with Th1 and Th2 immune responses (Fig. 4B). A special emphasis has been drawn to the genes linked with acute inflammatory response, TLR signaling, eosinophil migration, and cellular immunity (Table 1).

As expected from previous reports,[53,54] FI-RSV immunized mice displayed a strong and prolonged immune response with a mixture of Th1 and Th2 activities (Fig. 4A). The excessive production of cytokines that are involved in lung pathology and disease progression via the recruitment of eosinophils and induction of acute inflammatory response[13,55,56] was reported (Table 1). Although virus replication was markedly reduced ($10^{3.7}$ $TCID_{50}$/gram lung tissue), the histopathological findings further confirmed the effect of mice immunization with FI-RSV in the development of an acute inflammatory response in the lungs post-challenge. This was manifested by excessive cellular infiltration and obstruction of the bronchiolar lumen.

In another context, the primary infection model presented by mice immunized with empty pPOE vector showed a distinctive upregulation of Th-1 cytokines (Fig. 4A). A prolonged Th1-biased immune response in primary HRSV infection is well established.[25,53,57,58] The lung pathology was less severe than that reported in the FI-RSV immunized mice (Fig. 3B), although the lung viral load was still higher ($10^{5.6}$ $TCID_{50}$/gram lung tissue). From the aforementioned results, it can be suggested that the overproduction of Th2 cytokines, but not the virus itself, is responsible for pulmonary inflammation and disease progression. Conversely, the cytokine profile of mice immunized with pPOE-TF and pPOE-FM2 vectors and, to a lesser extent, with pPOE-F was significantly diminished by the 8th day post-challenge. In contrast to FI-RSV immunized mice, there was a marked increase in the fold change values of Th1-associated cytokines and downregulation of Th2-associated cytokines (Fig. 4A). This may reflect the ability of the immune system to control virus replication in the lungs, as confirmed by the reduced viral load to $10^{3.5}$, $10^{2.8}$ and $10^{3.0}$ $TCID_{50}$/gram lung tissue for pPOE-F, pPOE-TF and pPOE-FM2, respectively. Consequently, a less severe inflammatory response (Table 1) and leukocytic infiltration developed in lung tissue of these groups of mice (Fig. 3D, E and F).

Although DNA vaccines proved to be efficacious in small animal models, application of such vaccines to larger animals and humans is still a challenge. Weak immune response elicited by DNA vaccines in clinical trials downscored their significance in humans.[59] However, Wang et al, reported that DNA vaccination was safe and elicited protective CD8+ T cell responses in malaria-naïve human subjects.[60] Poor immune response due to DNA vaccines can be overcome by codon optimization of the transgene encoded by the vector, the use of built-in adjuvants and the delivery approaches.59 DNA vaccines can be considered for immunization of infants, the principle target for HRSV vaccination, for 2 reasons: 1) they do not interfere with the pre-existing maternal antibodies[61]; 2) a single dose is sufficient to elicit long-term immune response.[62] The built-in enhancers that were supplied in pPOE vector used in this study can provide an additional advantage for the use of this vector in infants. Despite the promising results obtained in BALB/c mice, further experiments are required to optimize the administration dose, the time intervals between doses, the administration route and the delivery approach. Similar studies are also essential to verify the extent and duration of immunity in other animal models like cotton rats and non-human primates.

In conclusion, findings of this study indicated that the 3 recombinant pPOE vectors; particularly pPOE-TF, were able to produce high titers of HRSV specific antibodies with neutralizing activity and robust CTL response. They protected mice from virus challenge as indicated by decreased viral load and histopathology score in lungs with cytokine expression profile close to negative controls. Overall, recombinant pPOE vectors are promising HRSV vaccine candidates for further evaluation in phase I clinical studies.

Materials and methods

Virus, cell culture and bacteria

HRSV type A strain Riyadh 91/2009[63] was propagated in human laryngeal epithelial (HEp-2) cells (ATCC, VA; CCL^{-}23) cultured in Dulbecco Modified Eagle's Medium (DMEM) (Invitrogen, 41966) with supplements including: 10% foetal bovine serum (FBS) (Invitrogen, 10270), 2 mM L-glutamine (Invitrogen, 25030), 100 U/ml penicillin, and 100 μg/ml streptomycin (Invitrogen 15240). A virus stock of 10^6 $TCID_{50}$/ml was prepared for use in the neutralization and challenge experiments. The virus stock was verified to be free from contamination with viral and/or bacterial pathogens using FTD respiratory pathogen 33 kit (Fast-track, FTD-2P-96/12). RAW 264.7 macrophage-like cells (ATCC) were cultured in DMEM with 10% FBS and penicillin/streptomycin. RAW macrophages were stimulated for 48 hours before use in the ^{51}Cr-release assays. For this purpose, cells were cultured in fresh medium supplemented with IFN-γ (20 ng/ml). Chemically competent *Escherichia coli* DH 10-β cells (DH-10–100, MCLAB) were used for high efficiency transformation of plasmid DNA by the heat shock method.

Generation of the immunization vectors

Three versions of the HRSV F gene (GenBank accession JF714710) were codon-optimized for the human system and synthesized by GenArt. These versions include the full-length F gene (F), the truncated F gene that lacks the trans-membrane domain (TF) and the full-length F gene with a downstream 27-nucleotide stretch [250–276] of the HRSV M2 gene (FM2) [GenBank accession numbers: KY432885-KY432887]. All versions were supplied with the Kozak sequence and the J-domain at the 5′-end and the SV40 enhancer sequence at the 3′-end (Fig. 1A). The different gene cassettes were cloned via 5′-*Hind*III (Thermo-Fisher, FD0504) and 3′-*Xba*I (Thermo-Fisher, FD0684) into the immunization vector pPOE,[30] which was originally derived from the vector pTHkan by inclusion of optimized CpG motifs for both the murine and human systems in the backbone[35] (Fig. 1B). Recombinant vectors were verified by sequencing and were designated as pPOE-F, pPOE-TF and pPOE-FM2.

In-vitro *expression analysis*

The expression potential of the recombinant immunization vectors was evaluated by transient reverse transfection of HEp-2 cells. Plasmid DNA was extracted using an EndoFree Plasmid Giga Kit (Qiagen, 12391). Preparations contained less than 0.1 endotoxin units/μg of plasmid DNA, as tested by the Limulus endotoxin assay, were incubated with lipofectamine® LTX reagent (Invitrogen, 15338–100) [1:6 w/v] for 5 minutes. The DNA/lipid complexes were added to 6-well plates in duplicates and covered by a suspension of HEp-2 cells (8×10^5/well). Cells transfected with pPOE vector or DNA-free mixture served as negative controls. After 48 hr of incubation, the expressed proteins were harvested using lysis buffer (1% Triton, 50 mM Tris-HCl; pH 7.4, 150 mM NaCl, 1 mM EDTA, 2 mM AEBSF, 1 mM Phosphoramidon, 130 mM Bestatin, 14 mM E-64, 1 mM Leupeptin, 0.2 mM Aprotinin, 10 mM Pepstatin A). Quantitative measurement of the expressed F protein was achieved using a human RSV fusion glycoprotein ELISA pair set (Sino Biological, SEK11049). The protein concentration was determined on the basis a reference curve for a known positive control recombinant fusion protein provided by the kit. In an independent transfection set, cells were fixed with 80% acetone and stained with anti-HRSV FITC-conjugated antibodies (ThermoFisher, PA1–73017). Fluorescence signals were recorded, and images were captured using an IN Cell analyzer 2000 (GE Healthcare).

Mice immunization and challenge

Female BALB/c mice (6–8 weeks old) were maintained under pathogen-free conditions at the animal facilities of the College of Pharmacy, King Saud University (KSU). The animal experiments were performed in accordance with the regulatory guidelines set by the Research Ethics Committee, KSU (4/67/352665). Two sets of the experiments were performed in parallel for validation of the results. BALB/c mice were divided into 6 groups (16 mice each) and immunized twice by means of an intramuscular injection at days 0 and 10. Four groups were immunized using 50 μg of pPOE, pPOE-F, pPOE-TF or pPOE-FM2 agarose verified plasmid vectors (> 95% supercoiled). The 5th group was immunized with saline (mock-immunized) and the 6th group with FI-RSV (3×10^5 pfu equivalents/mouse) for testing disease enhancement post-challenge.[13] Ten days after the second immunization, 4 mice were separated from each of the first 5 groups and killed for serum and spleen collection. The rest of the mice (n = 12) were intranasally challenged 4 d later with HRSV strain Riyadh 91/2009 (10^6 $TCID_{50}$/mouse). The mock-immunized group was challenged with saline only (mock-infected). Mice were monitored daily for signs of morbidity and mortality. Eight days post-challenge, all mice were killed, and the lungs were aseptically collected. The lungs of each group of mice were divided into 3 sets (4 lung pairs each) for separate use in the determination of viral load, histopathology and cytokine profile analysis. All operations on live animals were performed under Isoflurane anesthesia.

Analysis of serum antibodies

Sera collected from the immunized mice were tested for HRSV F-specific antibodies (IgG and IgA) by ELISA. Three μg/ml of recombinant F protein (ThermoFisher, 40039-V08B-50) diluted in PBS were used to coat round-bottom ELISA plates (Becton Dickinson) and plates were incubated at 4°C overnight. Incubated well containing PBS were used as negative controls to correct the absorbance value of each test sample. Plates were washed 3 times with PBS containing 0.05% Tween 20 (PBS-T) and incubated for 1 hr at 37°C with 100 μl of milk buffer (5% milk powder in PBS-T) per well. After 2 PBS washes, serum specimens (diluted 1:10 in milk buffer) were added and plates were incubated for 1 hr at 37°C. Samples were removed and washed 3 times with PBS. To detect IgGs, HRP-conjugated rabbit anti-mouse IgG (heavy and light chains) (ThermoFisher, 61–6520) diluted 1:3,000 were used. Serum IgAs were detected by the usage of HRP-conjugated goat anti-mouse IgA (Sigma-Aldrich, A4789) diluted 1:10,000. After incubation for 1 hr at 37°C and 3 washes with PBS, substrate (200 μg of tetramethylbenzidine per ml in a solution of 0.1 M Na acetate [pH 6.0] and 0.03% H_2O_2) was added. The reaction was stopped with 1 M H_2SO_4, and optical densities (ODs) were measured at 450 nm using a SpectraFluor Plus plate reader (Tecan, P97081). The neutralizing activity of the F-specific antibodies was determined as described before.[64] Briefly, 2-fold dilution series of sera samples (starting 1:10) were prepared in 96-well cell culture plates. Fifty microliters of Riyadh 91/2009 virus strain (100 $TCID_{50}$) were added to each well and incubated at 37°C for 1 hr. One-hundred microliters of HEp-2 cells (5×10^5 cells/mL) were added to each well and plates were incubated at 37°C/5% CO_2 till appearance of cytopathic effect (CPE) in virus control wells (5–7 days). The last well that showed a 100% inhibition of CPE formation was considered as the end point dilution of the serum sample. The neutralizing antibody titer was determined as the reciprocal of the end point serum dilution.

Determination of T cell responses

Two x 10^7 spleen cells (pre-treated with ACT lysis buffer [17 mM Tris/HCl, 160 mM NH_4Cl, pH 7.2] to deplete erythrocytes) were used directly for Elispot and ^{51}Cr-release assays. IFN-γ and granzyme B Elispot assays were performed *ex vivo* as described before.[65,66] Anti-mouse capture antibodies for IFN-γ

(200 ng/well; clone R4–6A2, BD Biosciences, 551216) or granzyme B (100 ng/well; R&D Systems, AF1865) were used to coat Multi-Screen-HA Filter Plates (Millipore, MAHAS4510). Splenocytes were seeded in triplicate in 2-fold dilutions from 2×10^5 to 2.5×10^4 cells/well. One of the triplicates was left untreated (negative control), the second received 200 ng of pokeweed mitogen/well (Sigma-Aldrich, L9379) in 2 μl of PBS (positive control), and the third received 0.2 μmol of KYKNAVTEL [F85–93, derived from F-protein of HRSV A2 strain] in 2 μl of PBS/well (test sample). After incubation for 16–20 hr at 37°C, cells were removed and biotinylated anti-mouse antibodies for IFN-γ (200 ng/well; clone XMG1.2, BD Biosciences, 554410) or granzyme B (50 ng/well; R&D Systems, BAF1865) were added and incubated at 4°C overnight. Streptavidin-alkaline phosphatase (diluted 1:1000 in PBS; BD Biosciences, 554065) was added after 3 successive washes and was left for 2 hr at RT. Spots were developed by adding 5-bromo-4-chloro-3-indolylphosphate/Nitro Blue Tetrazolium (Sigma-Aldrich, B5655). The reaction was stopped after 10 min, and spots were counted using a Zeiss Elispot reader. Counts of the negative control wells were subtracted from the counts of the test samples. The cytolytic activity of $CD8^+$ T cells was also determined after a single *in vitro* re-stimulation of murine splenocytes using a ^{51}Cr-release assay.[65] One x 10^4 $Na_2{}^{51}CrO_4$ labeled (0.05 mCi) peptide-loaded target cells/well (RAW cells, loaded with KYKNAVTEL [F85–93]) were incubated with decreasing numbers of effector cells in 200 μl per well of a 96-well round bottom plate (Costar, CLS3799) for 4 hr. Supernatants were harvested from individual wells for radioactivity measurements using a Microβ counter (Wallac). Specific lysis was calculated using the formula: % specific lysis = [(sample cpm – spontaneous release) / (total release – spontaneous release)] × 100, where the total and spontaneous release are measured in counts per minute (cpm).

Spontaneous chromium release was determined using ^{51}Cr-labeled target cells without effector cells, and total chromium release was determined by adding 2% Triton X-100 to lyse the labeled target cells.

Lung viral load

Lungs of challenged groups of mice were separately collected, weighed and homogenized. After centrifugation of tissue homogenates at 1000 xg for 30 min (4°C), the clarified supernatants were used for virus titration by an end point dilution assay. Ninety-six well plates with 70–90% confluent monolayers of HEp-2 cells were inoculated with a series of 10-fold dilutions of clarified lung supernatants (prepared in DMEM with 1% FBS and 1x antibiotics/antimycotics). Plates were incubated at 37°C and 5% CO_2 for 5–7 d before recording the cytopathological changes in the infected wells. Further confirmation of the results was achieved by staining another set of plates 48 hr after incubation using HRSV-specific FITC-conjugated antibodies and identification of the fluorescent signals using an IN Cell analyzer 2000. The lung virus titer was expressed as $TCID_{50}$/gm of lung tissue.

Histopathological examination

Lungs of 4 mice were collected from each group, rinsed and perfused with 10% neutral buffered formalin, and embedded in paraffin. Eight sections of each lung were prepared and stained with haematoxylin and eosin.[67] The lung sections were examined blindly, and 10 fields were read for each slide. The histopathological changes were evaluated using the scoring system developed by Hwang *et al.*,[24] A score of 0 was assigned when the surrounding space of bronchioles was free from infiltrating inflammatory cells. A score of 1 was assigned when the surrounding space of bronchioles was infiltrated with few inflammatory cells. A score of 2 was assigned when the surrounding space of bronchioles contained focal aggregates of infiltrating cells or the structure was cuffed by one layer of infiltrating cells. A score of 3 was assigned when the structure was cuffed by 2 or more layers of infiltrating cells with or without focal aggregates. Images were captured using an Eclipse E-800 microscope equipped with a DXM1200C digital camera (Nikon).

Pulmonary cytokine profiling for Th1 and Th2 responses

The expression of cytokines involved in Th1 and Th2 responses was evaluated in the lung tissue of immunized mice post-challenge. Lungs were homogenized in liquid nitrogen, and RNA was isolated using an RNeasy Mini Kit (Qiagen, 74104). cDNA synthesis and genomic DNA elimination were achieved using an RT^2 first strand synthesis kit (Qiagen, 330401). A mouse Th1 and Th2 RT^2-PCR Profiler Array (Qiagen, PAMM-034Z) was used to measure the expression level of 84 T-helper-associated genes in the ABI Prism 7500 Sequence Detection System (ThermoFisher). Five housekeeping genes (HKGs) and proprietary controls were tested in parallel for normalization of the assay results, monitoring genomic DNA contamination, cDNA synthesis and real-time PCR efficiency. Ct values were obtained using a constant baseline threshold, and the data were analyzed at a Qiagen data analysis center (http://www.qiagen.com/shop/genes-and-pathways/data-analysis-center-overview-page). A clustergram was generated to display heatmaps with dendrograms indicating co-regulated genes across groups using MORPHEUS software (https://software.broadinstitute.org/morpheus). Hierarchical clustering was built using one minus the Pearson's correlation value.

Statistical analysis

The data were presented as the means and standard deviations. Differences between groups were analyzed using Student's t-test (2-tailed). Probability values < 0.05 were considered significant.

Disclosure of potential conflicts of interest

No potential conflicts of interest were disclosed.

Funding

This project was supported by the NSTIP strategic technologies program (No. 14-MED809-02) in the Kingdom of Saudi Arabia.

References

[1] Nair H, Nokes DJ, Gessner BD, Dherani M, Madhi SA, Singleton RJ, O'Brien KL, Roca A, Wright PF, Bruce N, et al. Global burden of

acute lower respiratory infections due to respiratory syncytial virus in young children: a systematic review and meta-analysis. Lancet 2010; 375:1545-55; PMID:20399493; https://doi.org/10.1016/S0140-6736(10)60206-1

[2] Diez-Domingo J, Perez-Yarza EG, Melero JA, Sanchez-Luna M, Aguilar MD, Blasco AJ, Alfaro N, Lázaro P. Social, economic, and health impact of the respiratory syncytial virus: a systematic search. BMC Infect Dis 2014; 14:544; PMID:25358423; https://doi.org/10.1186/s12879-014-0544-x

[3] Bont L, Versteegh J, Swelsen WT, Heijnen CJ, Kavelaars A, Brus F, Draaisma JM, Pekelharing-Berghuis M, van Diemen-Steenvoorde RA, Kimpen JL. Natural reinfection with respiratory syncytial virus does not boost virus-specific T-cell immunity. Pediatr Res 2002; 52:363-7; PMID:12193668; https://doi.org/10.1203/00006450-200209000-00009

[4] Piedra PA. Clinical experience with respiratory syncytial virus vaccines. Pediatr Infect Dis J 2003; 22:S94-9; PMID:12671459

[5] Leader S, Kohlhase K. Recent trends in severe respiratory syncytial virus (RSV) among US infants, 1997 to 2000. J Pediatr 2003; 143:S127-32; PMID:14615711; https://doi.org/10.1067/S0022-3476(03)00510-9

[6] Falsey AR, Hennessey PA, Formica MA, Cox C, Walsh EE. Respiratory syncytial virus infection in elderly and high-risk adults. N Engl J Med 2005; 352:1749-59; PMID:15858184; https://doi.org/10.1056/NEJMoa043951

[7] Graham BS. Biological challenges and technological opportunities for respiratory syncytial virus vaccine development. Immunol Rev 2011; 239:149-66; PMID:21198670; https://doi.org/10.1111/j.1600-065X.2010.00972.x

[8] Rudraraju R, Jones BG, Sealy R, Surman SL, Hurwitz JL. Respiratory syncytial virus: current progress in vaccine development. Viruses 2013; 5:577-94; PMID:23385470; https://doi.org/10.3390/v5020577

[9] Afonso CL, Amarasinghe GK, Banyai K, Bao Y, Basler CF, Bavari S, Bejerman N, Blasdell KR, Briand FX, Briese T, et al. Taxonomy of the order Mononegavirales: update 2016. Arch Virol 2016; 161:2351-60; PMID:27216929; https://doi.org/10.1007/s00705-016-2880-1

[10] Collins PL, Huang YT, Wertz GW. Identification of a tenth mRNA of respiratory syncytial virus and assignment of polypeptides to the 10 viral genes. J Virol 1984; 49:572-8; PMID:6546401

[11] Levine S, Klaiber-Franco R, Paradiso PR. Demonstration that glycoprotein G is the attachment protein of respiratory syncytial virus. J Gen Virol 1987; 68(Pt 9):2521-4; PMID:3655746; https://doi.org/10.1099/0022-1317-68-9-2521

[12] Munoz FM, Piedra PA, Glezen WP. Safety and immunogenicity of respiratory syncytial virus purified fusion protein-2 vaccine in pregnant women. Vaccine 2003; 21:3465-7; PMID:12850361; https://doi.org/10.1016/S0264-410X(03)00352-9

[13] Rey GU, Miao C, Caidi H, Trivedi SU, Harcourt JL, Tripp RA, Anderson LJ, Haynes LM. Decrease in formalin-inactivated respiratory syncytial virus (FI-RSV) enhanced disease with RSV G glycoprotein peptide immunization in BALB/c mice. PLoS One 2013; 8:e83075; PMID:24376637; https://doi.org/10.1371/journal.pone.0083075

[14] Chin J, Magoffin RL, Shearer LA, Schieble JH, Lennette EH. Field evaluation of a respiratory syncytial virus vaccine and a trivalent parainfluenza virus vaccine in a pediatric population. Am J Epidemiol 1969; 89:449-63; PMID:4305200; https://doi.org/10.1093/oxfordjournals.aje.a120957

[15] Karron RA, Buchholz UJ, Collins PL. Live-attenuated respiratory syncytial virus vaccines. Curr Top Microbiol Immunol 2013; 372:259-84; PMID:24362694

[16] Lambert SL, Aslam S, Stillman E, MacPhail M, Nelson C, Ro B, Sweetwood R, Lei YM, Woo JC, Tang RS. A novel respiratory syncytial virus (RSV) F subunit vaccine adjuvanted with GLA-SE elicits robust protective TH1-type humoral and cellular immunity in rodent models. PLoS One 2015; 10:e0119509; PMID:25793508; https://doi.org/10.1371/journal.pone.0119509

[17] Kim E, Okada K, Beeler JA, Crim RL, Piedra PA, Gilbert BE, Gambotto A. Development of an adenovirus-based respiratory syncytial virus vaccine: preclinical evaluation of efficacy, immunogenicity, and enhanced disease in a cotton rat model. J Virol 2014; 88:5100-8; PMID:24574396; https://doi.org/10.1128/JVI.03194-13

[18] Moghaddam A, Olszewska W, Wang B, Tregoning JS, Helson R, Sattentau QJ, Openshaw PJ. A potential molecular mechanism for hypersensitivity caused by formalin-inactivated vaccines. Nat Med 2006; 12:905-7; PMID:16862151; https://doi.org/10.1038/nm1456

[19] Murphy BR, Hall SL, Kulkarni AB, Crowe JE, Jr, Collins PL, Connors M, Karron RA, Chanock RM. An update on approaches to the development of respiratory syncytial virus (RSV) and parainfluenza virus type 3 (PIV3) vaccines. Virus Res 1994; 32:13-36; PMID:8030364; https://doi.org/10.1016/0168-1702(94)90059-0

[20] Saade F, Petrovsky N. Technologies for enhanced efficacy of DNA vaccines. Expert Rev Vaccines 2012; 11:189-209; PMID:22309668; https://doi.org/10.1586/erv.11.188

[21] Wahren B, Liu MA. DNA Vaccines: recent developments and the future. vaccines 2014; 2:785-96; https://doi.org/10.3390/vaccines2040785

[22] Ternette N, Stefanou D, Kuate S, Uberla K, Grunwald T. Expression of RNA virus proteins by RNA polymerase II dependent expression plasmids is hindered at multiple steps. Virol J 2007; 4:51; PMID:17550613; https://doi.org/10.1186/1743-422X-4-51

[23] Stab V, Nitsche S, Niezold T, Storcksdieck Genannt Bonsmann M, Wiechers A, Tippler B, Hannaman D, Ehrhardt C, Uberla K, Grunwald T, et al. Protective efficacy and immunogenicity of a combinatory DNA vaccine against Influenza A Virus and the Respiratory Syncytial Virus. PLoS One 2013; 8:e72217; PMID:23967287; https://doi.org/10.1371/journal.pone.0072217

[24] Hwang HS, Kwon YM, Lee JS, Yoo SE, Lee YN, Ko EJ, Kim MC, Cho MK, Lee YT, Jung YJ, et al. Co-immunization with virus-like particle and DNA vaccines induces protection against respiratory syncytial virus infection and bronchiolitis. Antiviral Res 2014; 110:115-23; PMID:25110201; https://doi.org/10.1016/j.antiviral.2014.07.016

[25] Ko EJ, Kwon YM, Lee JS, Hwang HS, Yoo SE, Lee YN, Lee YT, Kim MC, Cho MK, Lee YR, et al. Virus-like nanoparticle and DNA vaccination confers protection against respiratory syncytial virus by modulating innate and adaptive immune cells. Nanomedicine 2015; 11:99-108; PMID:25109662

[26] Hwang HS, Lee YT, Kim KH, Park S, Kwon YM, Lee Y, Ko EJ, Jung YJ, Lee JS, Kim YJ, et al. Combined virus-like particle and fusion protein-encoding DNA vaccination of cotton rats induces protection against respiratory syncytial virus without causing vaccine-enhanced disease. Virology 2016; 494:215-24; PMID:27123586; https://doi.org/10.1016/j.virol.2016.04.014

[27] Wu H, Dennis VA, Pillai SR, Singh SR. RSV fusion (F) protein DNA vaccine provides partial protection against viral infection. Virus Res 2009; 145:39-47; PMID:19540885; https://doi.org/10.1016/j.virusres.2009.06.012

[28] Klinman DM. Adjuvant activity of CpG oligodeoxynucleotides. Int Rev Immunol 2006; 25:135-54; PMID:16818369; https://doi.org/10.1080/08830180600743057

[29] Barouch DH, Letvin NL, Seder RA. The role of cytokine DNAs as vaccine adjuvants for optimizing cellular immune responses. Immunol Rev 2004; 202:266-74; PMID:15546399; https://doi.org/10.1111/j.0105-2896.2004.00200.x

[30] Groettrup M, Oehlschlaeger P. Prostate cancer dna vaccine. U.S. Patent 2013/0115239, issued May 9, 2013.

[31] Bembridge GP, Rodriguez N, Garcia-Beato R, Nicolson C, Melero JA, Taylor G. DNA encoding the attachment (G) or fusion (F) protein of respiratory syncytial virus induces protection in the absence of pulmonary inflammation. J Gen Virol 2000; 81:2519-23; PMID:10993942; https://doi.org/10.1099/0022-1317-81-10-2519

[32] Ternette N, Tippler B, Uberla K, Grunwald T. Immunogenicity and efficacy of codon optimized DNA vaccines encoding the F-protein of respiratory syncytial virus. Vaccine 2007; 25:7271-9; PMID:17825960; https://doi.org/10.1016/j.vaccine.2007.07.025

[33] Barnum SB SP, Vig K, Pillai S, Dennis VA, Singh SR. Nano-Encapsulated DNA and/or Protein Boost Immunizations Increase Efficiency of DNA Vaccine Protection against RSV. J Nanomedic Nanotechnol 2012; 3:132

[34] Taylor G, Bruce C, Barbet AF, Wyld SG, Thomas LH. DNA vaccination against respiratory syncytial virus in young calves. Vaccine 2005; 23:1242-50; PMID:15652666; https://doi.org/10.1016/j.vaccine.2004.09.005

[35] Ohlschlager P, Spies E, Alvarez G, Quetting M, Groettrup M. The combination of TLR-9 adjuvantation and electroporation-mediated delivery enhances *in vivo* antitumor responses after vaccination with HPV-16 E7 encoding DNA. Int J Cancer 2011; 128:473-81; PMID:20309939; https://doi.org/10.1002/ijc.25344

[36] Spies E, Reichardt W, Alvarez G, Groettrup M, Ohlschlager P. An artificial PAP gene breaks self-tolerance and promotes tumor regression in the TRAMP model for prostate carcinoma. Mol Ther 2012; 20:555-64; https://doi.org/10.1038/mt.2011.241

[37] Lee S, Stokes KL, Currier MG, Sakamoto K, Lukacs NW, Celis E, Moore ML. Vaccine-elicited CD8+ T cells protect against respiratory syncytial virus strain A2-line19F-induced pathogenesis in BALB/c mice. J Virol 2012; 86:13016-24; PMID:23015695; https://doi.org/10.1128/JVI.01770-12

[38] Coll RC, O'Neill LA. New insights into the regulation of signalling by toll-like receptors and nod-like receptors. J Innate Immun 2010; 2:406-21; PMID:20505309; https://doi.org/10.1159/000315469

[39] Tachibana R, Harashima H, Shinohara Y, Kiwada H. Quantitative studies on the nuclear transport of plasmid DNA and gene expression employing nonviral vectors. Adv Drug Deliv Rev 2001; 52:219-26; PMID:11718946; https://doi.org/10.1016/S0169-409X(01)00211-3

[40] Li PP, Nakanishi A, Shum D, Sun PC, Salazar AM, Fernandez CF, Chan SW, Kasamatsu H. Simian virus 40 Vp1 DNA-binding domain is functionally separable from the overlapping nuclear localization signal and is required for effective virion formation and full viability. J Virol 2001; 75:7321-9; PMID:11462004; https://doi.org/10.1128/JVI.75.16.7321-7329.2001

[41] Kim NY, Chang DS, Kim Y, Kim CH, Hur GH, Yang JM, Shin S. Enhanced Immune Response to DNA Vaccine Encoding Bacillus anthracis PA-D4 protects mice against Anthrax Spore challenge. PLoS One 2015; 10:e0139671; PMID:26430894; https://doi.org/10.1371/journal.pone.0139671

[42] Costello HM, Ray WC, Chaiwatpongsakorn S, Peeples ME. Targeting RSV with vaccines and small molecule drugs. Infect Disord Drug Targets 2012; 12:110-28; PMID:22335496; https://doi.org/10.2174/187152612800100143

[43] Cobleigh MA, Wei X, Robek MD. A vesicular stomatitis virus-based therapeutic vaccine generates a functional CD8 T cell response to hepatitis B virus in transgenic mice. J Virol 2013; 87:2969-73; PMID:23269785; https://doi.org/10.1128/JVI.02111-12

[44] Slon Campos JL, Poggianella M, Marchese S, Bestagno M, Burrone OR. Secretion of dengue virus envelope protein ectodomain from mammalian cells is dependent on domain II serotype and affects the immune response upon DNA vaccination. J Gen Virol 2015; 96:3265-79; PMID:26358704; https://doi.org/10.1099/jgv.0.000278

[45] Kulkarni AB, Connors M, Firestone CY, Morse HC, 3rd, Murphy BR. The cytolytic activity of pulmonary CD8+ lymphocytes, induced by infection with a vaccinia virus recombinant expressing the M2 protein of respiratory syncytial virus (RSV), correlates with resistance to RSV infection in mice. J Virol 1993; 67:1044-9; PMID:8419638

[46] Begona Ruiz-Arguello M, Gonzalez-Reyes L, Calder LJ, Palomo C, Martin D, Saiz MJ, García-Barreno B, Skehel JJ, Melero JA. Effect of proteolytic processing at two distinct sites on shape and aggregation of an anchorless fusion protein of human respiratory syncytial virus and fate of the intervening segment. Virology 2002; 298:317-26; PMID:12127793; https://doi.org/10.1006/viro.2002.1497

[47] Krarup A, Truan D, Furmanova-Hollenstein P, Bogaert L, Bouchier P, Bisschop IJ, Widjojoatmodjo MN, Zahn R, Schuitemaker H, McLellan JS, et al. A highly stable prefusion RSV F vaccine derived from structural analysis of the fusion mechanism. Nat Commun 2015; 6:8143; PMID:26333350; https://doi.org/10.1038/ncomms9143

[48] McLellan JS, Yang Y, Graham BS, Kwong PD. Structure of respiratory syncytial virus fusion glycoprotein in the postfusion conformation reveals preservation of neutralizing epitopes. J Virol 2011; 85:7788-96; PMID:21613394; https://doi.org/10.1128/JVI.00555-11

[49] Cimica V, Boigard H, Bhatia B, Fallon JT, Alimova A, Gottlieb P, Galarza JM. Novel Respiratory Syncytial Virus-Like Particle Vaccine Composed of the Postfusion and Prefusion Conformations of the F Glycoprotein. Clin Vaccine Immunol 2016; 23:451-9; PMID:27030590; https://doi.org/10.1128/CVI.00720-15

[50] Lee JS, Kwon YM, Hwang HS, Lee YN, Ko EJ, Yoo SE, Kim MC, Kim KH, Cho MK, Lee YT, et al. Baculovirus-expressed virus-like particle vaccine in combination with DNA encoding the fusion protein confers protection against respiratory syncytial virus. Vaccine 2014; 32:5866-74; PMID:25173478; https://doi.org/10.1016/j.vaccine.2014.08.045

[51] Chang J, Srikiatkhachorn A, Braciale TJ. Visualization and characterization of respiratory syncytial virus F-specific CD8(+) T cells during experimental virus infection. J Immunol 2001; 167:4254-60; PMID:11591747; https://doi.org/10.4049/jimmunol.167.8.4254

[52] Farrag MA, Almajhdi FN. Human respiratory syncytial virus: Role of innate immunity in clearance and disease progression. Viral Immunol 2016; 29:11-26; PMID:26679242; https://doi.org/10.1089/vim.2015.0098

[53] Schuurhof A, Bont L, Pennings JL, Hodemaekers HM, Wester PW, Buisman A, de Rond LC, Widjojoatmodjo MN, Luytjes W, Kimpen JL, et al. Gene expression differences in lungs of mice during secondary immune responses to respiratory syncytial virus infection. J Virol 2010; 84:9584-94; PMID:20592085; https://doi.org/10.1128/JVI.00302-10

[54] Su YC, Townsend D, Herrero LJ, Zaid A, Rolph MS, Gahan ME, Nelson MA, Rudd PA, Matthaei KI, Foster PS, et al. Dual proinflammatory and antiviral properties of pulmonary eosinophils in respiratory syncytial virus vaccine-enhanced disease. J Virol 2015; 89:1564-78; PMID:25410867; https://doi.org/10.1128/JVI.01536-14

[55] Dou Y, Zhao Y, Zhang ZY, Mao HW, Tu WW, Zhao XD. Respiratory syncytial virus infection induces higher Toll-like receptor-3 expression and TNF-alpha production than human metapneumovirus infection. PLoS One 2013; 8:e73488; PMID:24039959; https://doi.org/10.1371/journal.pone.0073488

[56] Knudson CJ, Varga SM. The relationship between respiratory syncytial virus and asthma. Vet Pathol 2015; 52:97-106; PMID:24513802; https://doi.org/10.1177/0300985814520639

[57] Lee YT, Kim KH, Hwang HS, Lee Y, Kwon YM, Ko EJ, Jung YJ, Lee YN, Kim MC, Kang SM. Innate and adaptive cellular phenotypes contributing to pulmonary disease in mice after respiratory syncytial virus immunization and infection. Virology 2015; 485:36-46; PMID:26196232; https://doi.org/10.1016/j.virol.2015.07.001

[58] Schmidt MR, McGinnes LW, Kenward SA, Willems KN, Woodland RT, Morrison TG. Long-term and memory immune responses in mice against Newcastle disease virus-like particles containing respiratory syncytial virus glycoprotein ectodomains. J Virol 2012; 86:11654-62; PMID:22896618; https://doi.org/10.1128/JVI.01510-12

[59] Ferraro B, Morrow MP, Hutnick NA, Shin TH, Lucke CE, Weiner DB. Clinical applications of DNA vaccines: current progress. Clin Infect Dis 2011; 53:296-302; PMID:21765081; https://doi.org/10.1093/cid/cir334

[60] Wang R, Doolan DL, Le TP, Hedstrom RC, Coonan KM, Charoenvit Y, Jones TR, Hobart P, Margalith M, Ng J, et al. Induction of antigen-specific cytotoxic T lymphocytes in humans by a malaria DNA vaccine. Science 1998; 282:476-80; PMID:9774275; https://doi.org/10.1126/science.282.5388.476

[61] Premenko-Lanier M, Rota PA, Rhodes GH, Bellini WJ, McChesney MB. Protection against challenge with measles virus (MV) in infant macaques by an MV DNA vaccine administered in the presence of neutralizing antibody. J Infect Dis 2004; 189:2064-71; PMID:15143474; https://doi.org/10.1086/420792

[62] Hassett DE, Zhang J, Slifka M, Whitton JL. Immune responses following neonatal DNA vaccination are long-lived, abundant, and qualitatively similar to those induced by conventional immunization. J Virol 2000; 74:2620-7; PMID:10684276; https://doi.org/10.1128/JVI.74.6.2620-2627.2000

[63] Almajhdi FN, Farrag MA, Amer HM. Genetic diversity in the G protein gene of group A human respiratory syncytial viruses circulating in Riyadh, Saudi Arabia. Arch Virol 2014; 159:73-81; PMID:23884633; https://doi.org/10.1007/s00705-013-1792-6

[64] Gauger PC, Vincent AL. Serum virus neutralization assay for detection and quantitation of serum-neutralizing antibodies to influenza A virus in swine. Methods Mol Biol 2014; 1161:313-24; PMID:24899440

[65] Almajhdi FN, Senger T, Amer HM, Gissmann L, Ohlschlager P. Design of a highly effective therapeutic HPV16 E6/E7-specific DNA vaccine: optimization by different ways of sequence rearrangements (shuffling). PLoS One 2014; 9:e113461; PMID:25422946; https://doi.org/10.1371/journal.pone.0113461

[66] Ohlschlager P, Pes M, Osen W, Durst M, Schneider A, Gissmann L, Kaufmann AM. An improved rearranged Human Papillomavirus Type 16 E7 DNA vaccine candidate (HPV-16 E7SH) induces an E7 wildtype-specific T cell response. Vaccine 2006; 24:2880-93; PMID:16472545; https://doi.org/10.1016/j.vaccine.2005.12.061

[67] Murawski MR, McGinnes LW, Finberg RW, Kurt-Jones EA, Massare MJ, Smith G, Heaton PM, Fraire AE, Morrison TG. Newcastle disease virus-like particles containing respiratory syncytial virus G protein induced protection in BALB/c mice, with no evidence of immunopathology. J Virol 2010; 84:1110-23; PMID:19889768; https://doi.org/10.1128/JVI.01709-09